Electronic Supplementary Information

Amide-based small molecule as hole transporting material for solid-state dye-sensitised solar cells

Amy Neild[a], Owen Woodford[a], Pablo Docampo[b], and Elizabeth A. Gibson[a]*

[a]Energy Materials Laboratory, Chemistry, School of Natural and Environmental Sciences, Bedson Building, Newcastle University, Newcastle upon Tyne, NE1 7RU, UK.
elizabeth.gibson@newcastle.ac.uk

[b]Basque Centre for Materials, Nanostructures and Applications, Leioa 48940, Spain
pablo.docampo@bcmaterials.net

Experimental Section

Chemical Reagents. All chemicals were used as received without further purification. Titanium(IV) isopropoxide (97%), acetylacetone (≥99%), transparent titania paste, titanium(IV) chloride tetrahydrofuran complex (97%), tert-Butanol (≥99.5%), acetonitrile (≥99.9%), spiro-OMeTAD (99%), and tBP (98%) were purchased from Sigma-Aldrich. Ethanol (99.8%) was purchased from Fisher Chemicals. LEG4 (DN-F05) was purchased from Dyenamo. Anhydrous chlorobenzene (99.5%, extra dry), anhydrous chloroform (99.9%, extra dry), anhydrous isopropanol (99.8%, extra dry), and LiTFSI (99%) were purchased from Acros Organics. Anhydrous acetonitrile (>99.8%) was purchased from Alfa Aesar.

Device Fabrication. Fluorine-doped tin oxide (FTO, Pilkington, 7 Ω sq^{-1}) coated glass substrates were cleaned in ultrasonic baths of detergent diluted in tap water (15 min), de-ionised water (15 min), and ethanol (15 min) in sequence. The substrates were then blown dry using a nitrogen flow. The FTO was then etched using a Ulyxe laser etcher to create the electrode pattern and then exposed to UV-ozone for 15 min to remove the last traces of organic residues. A compact TiO_2 blocking layer was deposited via 15 spray cycles of spray pyrolysis on a hotplate at 450°C using an airbrush and N_2 as the carrier gas. The solution used in the spray pyrolysis was 3.6 ml acetylacetone and 2.4 ml titanium(IV) isopropoxide dissolved in 54 ml ethanol. To deposit the mesoporous TiO_2 film (~ 1.9 µm), transparent titania paste was screen printed onto the compact layer. After sintering on a hotplate at 450°C for 30 min the substrates were cooled to room temperature and immersed into a 40 mM aqueous solution of titanium(IV) chloride tetrahydrofuran complex for 20 min at 70°C. The substrates were then rinsed with de-ionised water and ethanol successively, and then annealed on a hotplate at 500°C for 30 min. Once cooled to 70°C the substrates were immersed into a 0.1 mM solution of LEG4 sensitiser in a mixture of tert-butanol and acetonitrile (1:1 volume ratio). The substrates were left in the solution for

16 h and then the sensitised electrodes were rinsed with acetonitrile. The preparation and deposition of the HTM solutions were carried out in a nitrogen-filled glovebox. The HTM solution was homogeneously spread by a pipette onto the sensitised electrode and left to penetrate into the mesoporous network for 30 s, followed by a two-step spin coating for 40 s at 700 rpm then 2 s at 2000 rpm. The films were left overnight in a desiccator. The substrates were placed in a BOC-Edwards Auto thermal evaporator where 120 nm of silver was deposited through a mask under high vacuum (10^{-6} Torr) at a rate of 1 $Å s^{-1}$ to form the silver electrodes.

Hole Transporting Material Deposition. The formulation of the Spiro-OMeTAD HTM solution was 100 mg ml^{-1} Spiro-OMeTAD in anhydrous chlorobenzene, with the addition of 76 mM tBP and 25 mM LiTFSI (LiTFSI was pre-dissolved in acetonitrile at 170 mg ml^{-1}). The solution was filtered through a 0.45 µm PTFE syringe filter and 50 µl was dispensed onto the substrate. The formulation of the TPABT HTM was 50 mg ml^{-1} TPABT (synthesised as previously reported)[1] dissolved in a mixture of anhydrous chloroform and anhydrous chlorobenzene (2:1 volume ratio) along with various concentrations of LiTFSI and tBP (concentrations are specified in figure captions). The TPABT solution was heated for 10 min at 70°C until transparent, then passed hot through a 0.45 µm PTFE syringe filter and 60 µl was dispensed onto the substrate.

Device Characterisation. Ultraviolet-Visible (UV-Vis) spectroscopy measurements were taken using an Ocean Optics USB2000+ Fiber Optic Spectrometer. Current Density vs Voltage (J-V) measurements were taken using a Keysight U2722A source meter with a HelioSim-CL60 solar simulator (Voss electronic GmbH). Reported photovoltaic parameters correspond to the best-performing pixels and were obtained from the reverse scan (open circuit to short circuit) of the J-V measurement. Photoinduced Absorption (PIA) Spectroscopy measurements were taken using square-wave-modulated (Signal Recovery 650) blue light (405 nm, 3 mW, Thorlabs) for excitation, while as a probe a white light (ASB-W-030 Spectral Products) was used, which focussed on a monochromator (Digikröm CM110). A circular photodiode (Thorlabs) initially recorded a DC±AC signal, which was amplified and split into its components using a pre-amplifier (Model 5182 Signal Recovery). The lock-in amplifier (Model 7225 Signal Recovery) locked onto the reference phase from the chopper unit and extracted amplitude and phase of the AC signal. External Quantum Efficiency (EQE) and Internal Quantum Efficiency (IQE) were recorded using a Bentham PV characterisation system. Scanning Electron Microscopy (SEM) was performed using a JSM-IT510 InTouchScope Microscope.

Transient Absorption Spectroscopy. Experiments were conducted using a Helios spectrometer from Ultrafast Systems, with a Solstice Ace laser (Spectra Physics) generating pump and probe beams. The laser produced pulses of 800 nm light with a duration of 100 fs at 1 kHz which was passed through a

sapphire crystal to form a white light continuum. The pump light was tuned to the desired wavelength using an optical parametric amplifier (OPA) model Apollo-T from Ultrafast Systems. Spectra were recorded using a fibre-coupled CCD array. Excitation of 490 nm was used with a pump power of 60 µW. The pump power was varied to check for linearity and minimised to limit dye photobleaching. Four spectra were taken per sample and averaged to achieve the presented spectra. Analysis was performed using Surface Xplorer.

Results

Scanning Electron Microscopy

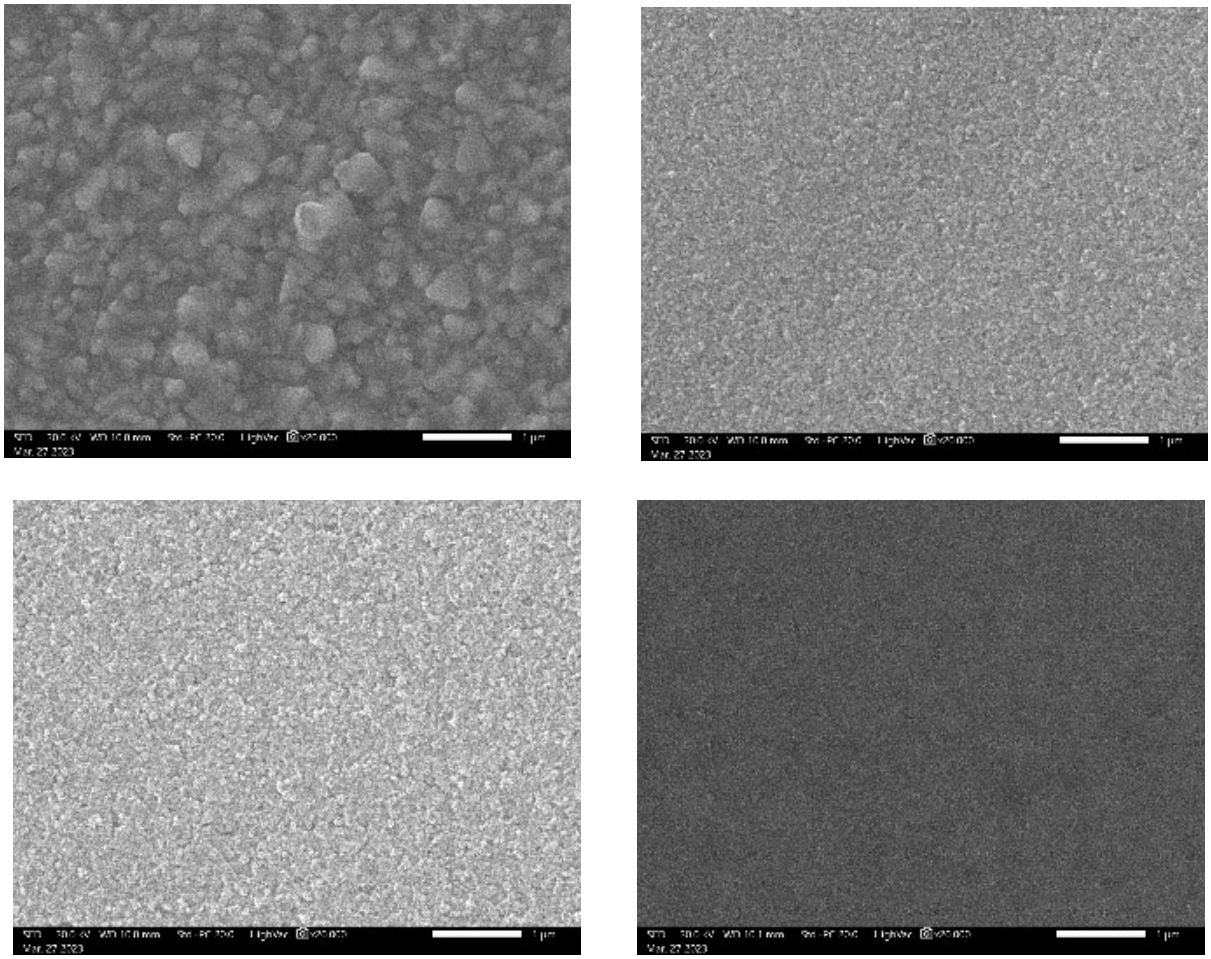

Figure S1. From top left to bottom right: FTO; FTO+TiO_2; FTO+TiO_2+LEG4; FTO+TiO_2+LEG4+TPABT measured at TPABT × 20,000. included 50 mg ml^{-1} TPABT, 75 mM LiTFSI and 76 mM tBP. Scale bar represents 1 µm.

ssDSSC characterisation

Table S1. Molar concentrations of the additives tBP and Li-TFSI to 50 mg ml^{-1} TPABT for two sets of samples (S and T, where S = 114:38 mM and uses the tBP:Li-TFSI ratio 1:0.33, and T = 114:25 and uses the ratio 1:0.22). Photo conversion efficiency (PCE) for reverse and forward scans are included.

Units of additive	**tBP (mM)**	**Li-TFSI (mM)**	**Reverse scan PCE (%)**	**Forward scan PCE (%)**
S1	114	38	0.047	**0.046**
S2	228	76	0.226	**0.044**
S3	342	114	0.175	**0.025**
S4	456	152	0.189	**0.017**
S5	570	190	0.189	**0.007**
T1	114	25	0.018	**0.012**
T2	228	50	0.070	**0.021**
T3	342	75	0.222	**0.052**
T4	456	100	0.238	**0.036**
T5	570	125	0.154	**0.026**

Table S2: JV characteristics measured from forward and reverse scans for devices with increasing concentration of LiTFSI, with 76 mM tBP for all.

Li-TFSI (mM)	**Reverse scan Jsc (mA cm^{-2})**	**Forward scan Jsc (mA cm^{-2})**	**Reverse scan PCE (%)**	**Forward scan PCE (%)**	**Reverse scan Voc (V)**	**Forward scan Voc (V)**	**Reverse scan FF**	**Forward scan FF**
25	0.44	**0.47**	0.14	**0.13**	0.87	**0.83**	0.37	**0.34**
50	0.26	**0.28**	0.14	**0.11**	0.86	**0.86**	0.61	**0.44**
75	0.31	**0.32**	0.19	**0.05**	0.76	**0.63**	0.80	**0.26**
100	-0.03	**-0.01**	0.02	**0.01**	0.98	**0.77**	0.76	**2.74**

Table S3: Device characteristics for the first series of FTO|TiO_2|LEG4|HTM|Ag ssDSSCs with (50 mg ml^{-1} TPABT, 76 mM LiTFSI and 228 mM tBP (S2), and 75 mM LiTFSI and 342 mM tBP (T3)) and Spiro-OMeTAD (25 mM LiTFSI and 76 mM tBP and 100 mg ml^{-1} Spiro-OMeTAD) measured after (a) 2 days (fresh) and (b) 3 months storage in an air filled desiccator (oxidation), (c) 3 months storage in an air filled desiccator after light soaking. V_{OC} = the open circuit voltage, J_{SC} = short circuit current density, FF = fill factor, PCE = solar to electrical power conversion efficiency.

Sample	**Fresh sample**				**After oxidation**				**After light soaking**			
	V_{OC} (V)	J_{SC} (mA cm^{-2})	FF	PCE (%)	V_{OC} (V)	J_{SC} (mA cm^{-2})	FF	PCE (%)	V_{OC} (V)	J_{SC} (mA cm^{-2})	FF	PCE (%)
Spiro (reference)	0.82	7.05	0.68	3.78	0.88	6.89	0.43	2.49	0.84	7.14	0.53	3.03
S2 – 228 mM tBP	0.69	0.31	0.20	0.04	0.65	2.12	0.42	0.58	0.71	4.93	0.65	2.26
T3 – 342 mM tBP	0.64	0.10	0.37	0.02	0.67	4.75	0.39	1.22	0.68	4.63	0.58	1.83

Table S4. Device characteristics for a second series of FTO|TiO_2|LEG4|HTM|Ag ssDSSCs with TPABT (76 mM tBP, 50 mg ml^{-1} TPABT and different concentrations LiTFSI: 25 mM - 100 mM) and Spiro-OMeTAD (25 mM LiTFSI and 76 mM tBP and 100 mg ml^{-1} Spiro-OMeTAD) measured after (a) 2 days (fresh) and (b) 3 months storage in an air filled desiccator (oxidation), (c) 3 months storage in an air filled desiccator after light soaking. V_{OC} = the open circuit voltage, J_{SC} = short circuit current density, FF = fill factor, PCE = solar to electrical power conversion efficiency. Asterisks denote non-physical FF values (>1), indicative of significant hysteresis or non-working cells.

Sample	**Fresh sample**				**After oxidation**				**After light soaking**			
	V_{OC} (V)	J_{SC} (mA cm^{-2})	FF	PCE (%)	V_{OC} (V)	J_{SC} (mA cm^{-2})	FF	PCE (%)	V_{OC} (V)	J_{SC} (mA cm^{-2})	FF	PCE (%)
TPABT – 25 mM LiTFSI	0.83	0.47	0.34	0.13	0.78	0.39	0.39	0.12	0.81	0.65	0.40	0.21
TPABT – 50 mM LiTFSI	0.87	0.32	0.39	0.11	0.86	0.22	0.36	0.07	0.85	0.13	0.33	0.04
TPABT – 75 mM LiTFSI	0.68	0.21	0.33	0.05	0.70	0.95	0.49	0.33	0.73	5.11	0.40	1.48
TPABT – 100 mM LiTFSI	0.72	-0.06	0.28	0.01	*0.71*	*-4.0x10^{-3}*	*3.34**	*0.01*	*0.22*	*4.0x10^{-3}*	*20.9**	*0.02*

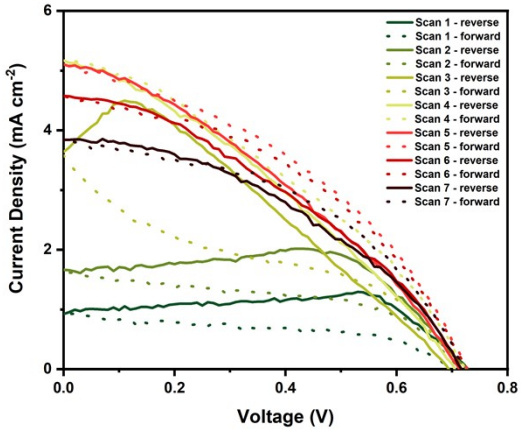

Figure S2. Successive J-V curves for 3 month aged FTO|TiO_2|LEG4|TPABT|Ag ssDSSC with 75 mM LiTFSI and 76 mM tBP additives to 50 mg ml^{-1} TPABT, showing a significant reduction in hysteresis and improvement of device performance with successive scans. Devices were measured under AM1.5 simulated sun light of 100 mW cm^{-2} irradiance at 0.1 V s^{-1}.

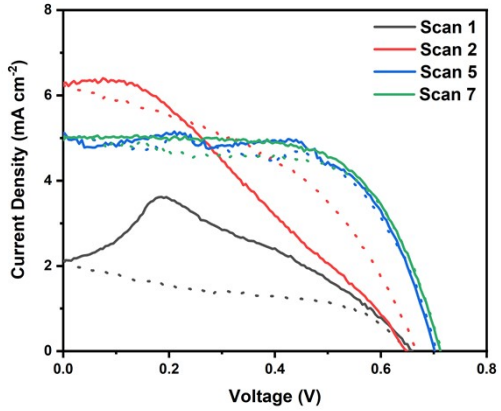

Figure S3. Successive J-V curves for 3 month aged FTO|TiO_2|LEG4|TPABT|Ag ssDSSC with 75 mM LiTFSI and 228 mM tBP additives to 50 mg ml^{-1} TPABT, showing a significant reduction in hysteresis and improvement of device performance with successive scans. Devices were measured under AM1.5 simulated sun light of 100 mW cm^{-2} irradiance at 0.1 V s^{-1}.

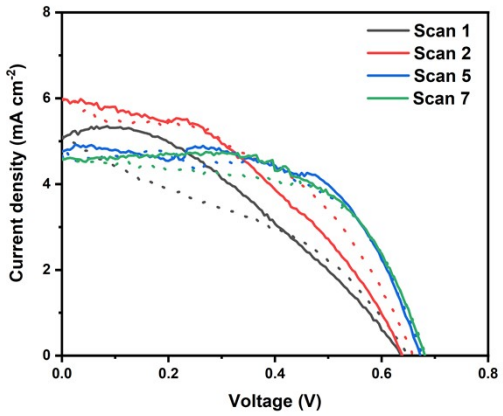

Figure S4. Successive J-V curves for 3 month aged FTO|TiO_2|LEG4|TPABT|Ag ssDSSC with 75 mM LiTFSI and 342 mM tBP additives to 50 mg ml^{-1} TPABT, showing a significant reduction in hysteresis and improvement of device performance with successive scans. Devices were measured under AM1.5 simulated sun light of 100 mW cm^{-2} irradiance at 0.1 V s^{-1}.

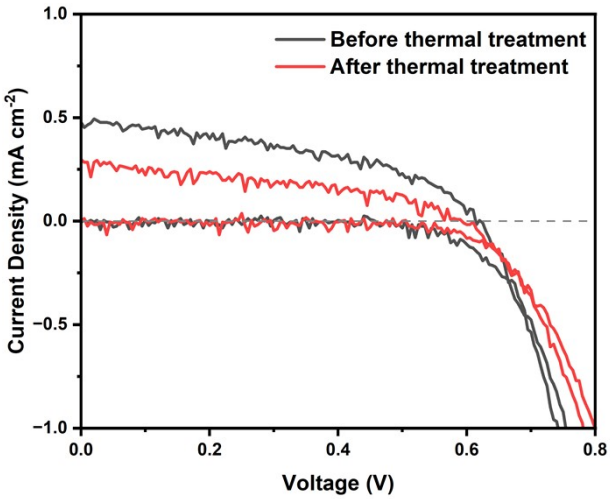

Figure S5. FTO|TiO_2|LEG4|TPABT|Ag ssDSSC with 75 mM LiTFSI and 76 mM tBP additives to 50 mg ml^{-1} TPABT, measured before and after thermal treatment at 60 °C in the dark for 10 minutes. This shows that increase in efficiency is not due to the temperature increase of the cell.

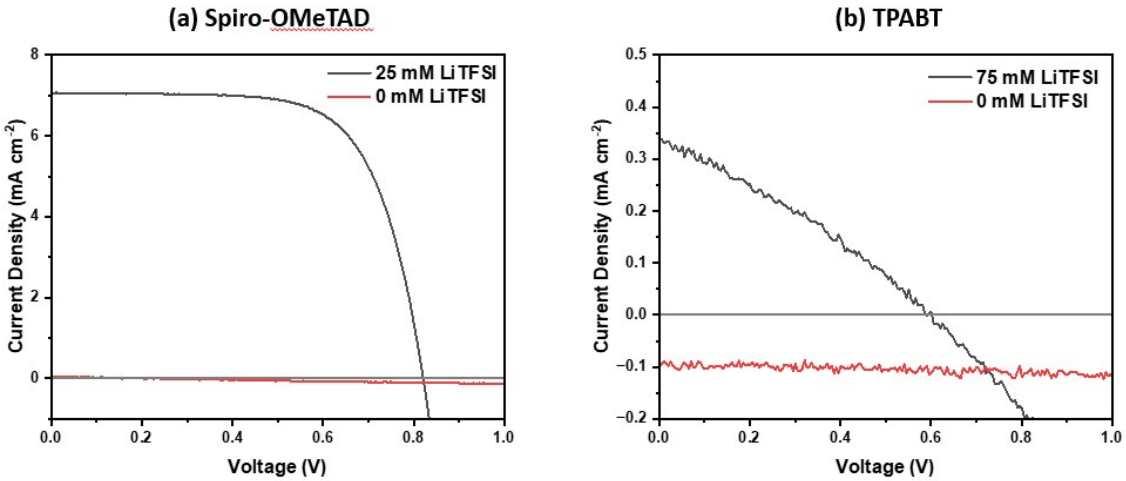

Figure S6. Light-soaked FTO|TiO_2|LEG4|HTM|Ag ssDSSC with (a) Spiro-OMeTAD (76 mM tBP and 100 mg ml^{-1} Spiro-OMeTAD) with 0 mM LiTFSI (red) and 25 mM LiTFSI (black) and (b) TPABT (76 mM tBP and 50 mg ml^{-1} TPABT) with 0 mM LiTFSI (red) and 75 mM LiTFSI (black). Devices without LiTFSI exhibited no measurable photovoltaic response. This shows that the cells do not operate as functioning ssDSSCs in the absence of LiTFSI.

Internal and external quantum efficiency

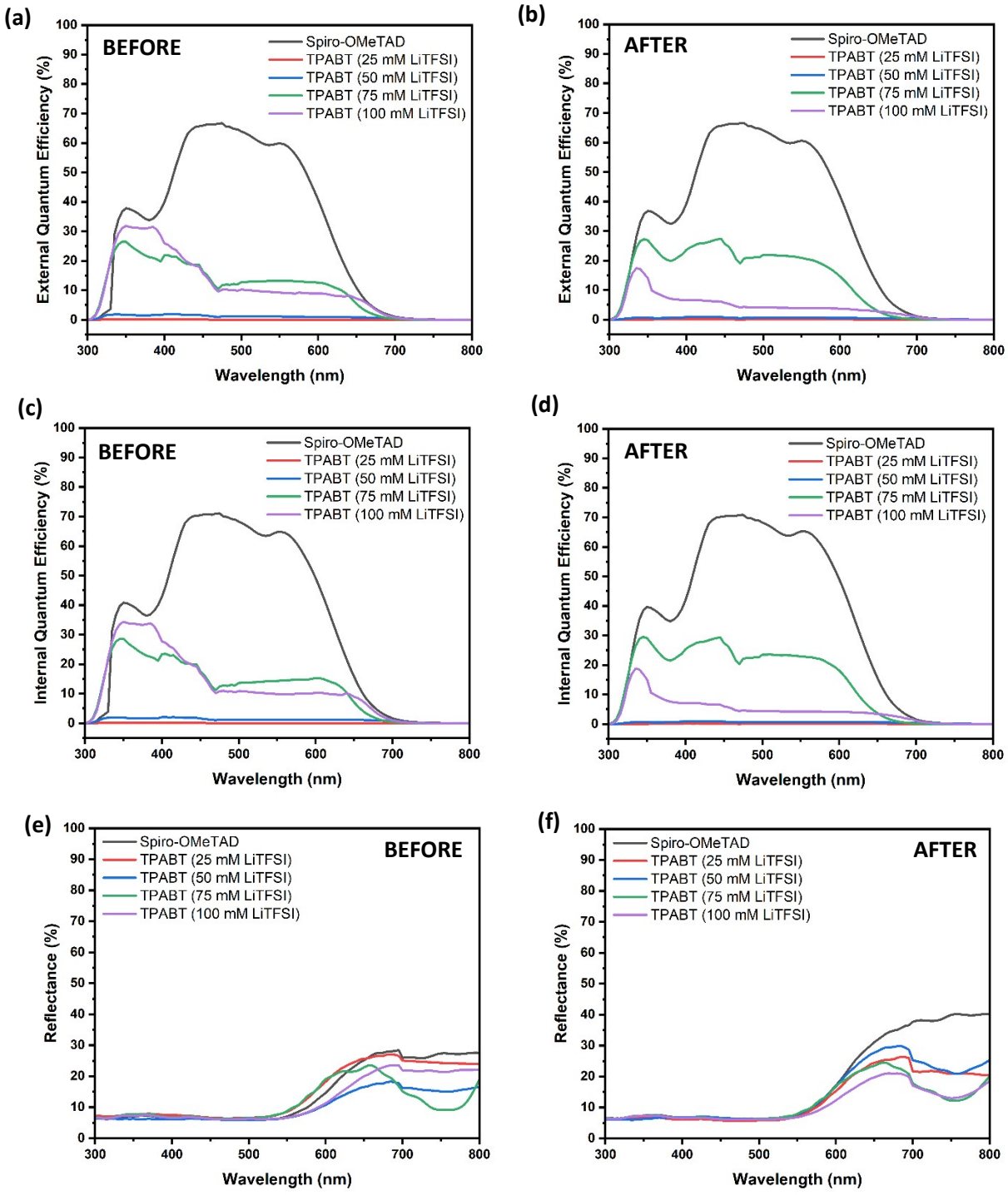

Figure S7. External quantum efficiency (a) before and (b) after light soaking. Internal quantum efficiency (c) before and (d) after light soaking. Reflectance (e) before and (f) after light soaking. TPABT devices are partially oxidised. Devices are FTO|TiO_2|LEG4|HTM|Ag ssDSSC with TPABT (50 mg ml^{-1} TPABT, 76 mM LiTFSI and 228 mM tBP (red), and 75 mM LiTFSI and 342 mM tBP (blue)) and Spiro-OMeTAD (25 mM LiTFSI and 76 mM tBP and 100 mg ml^{-1} Spiro-OMeTAD (black)).

UV-visible Absorption Spectroscopy

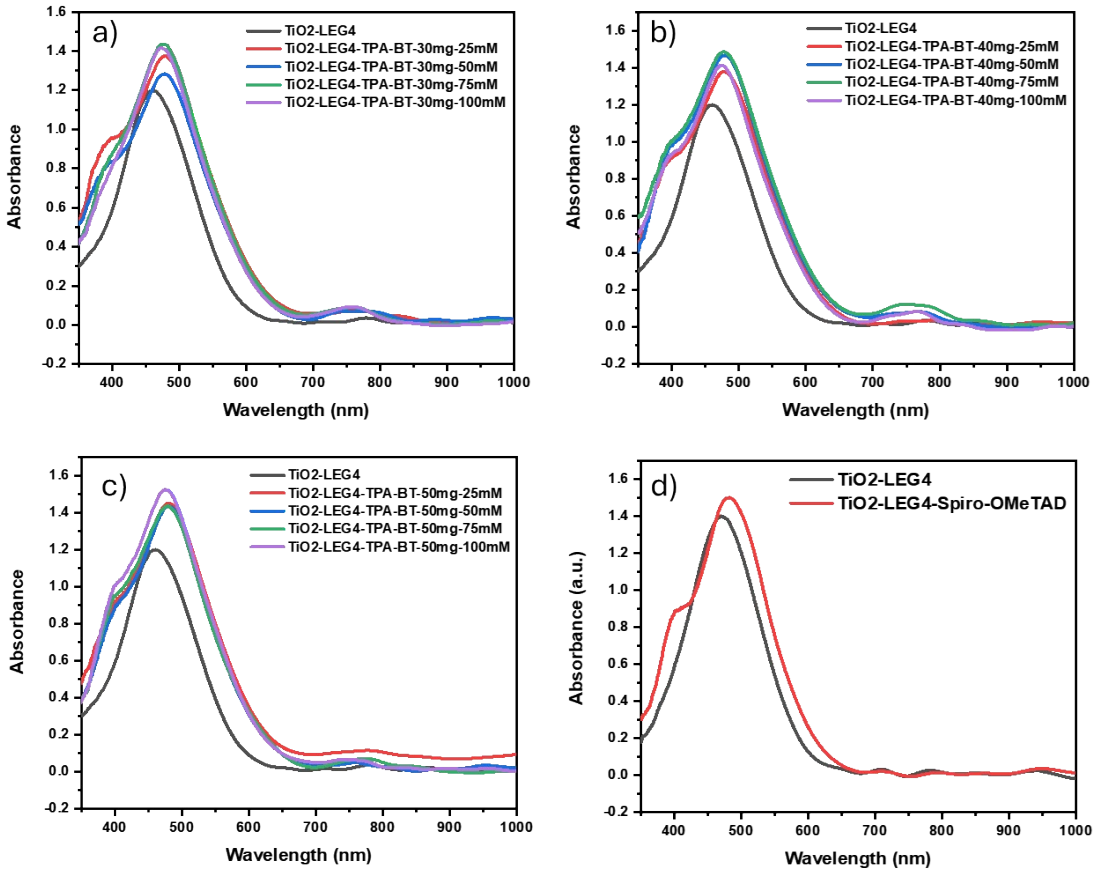

Figure S8 UV-Vis spectra of TiO_2|LEG4|TPABT samples on FTO glass with varying concentration of Li-TFSI added to TPABT and 76 mM tBP, for TPABT concentrations of a) 30 mg ml^{-1}, b) 40 mg ml^{-1} and c) 50 mg ml^{-1} and d) for TiO_2|LEG4|Spiro-OMeTAD on samples of FTO glass with 25 mM LiTFSI, 76 mM tBP and 100 mg ml^{-1} Spiro-OMeTAD. The spectrum for the mesoporous TiO_2 film was subtracted.

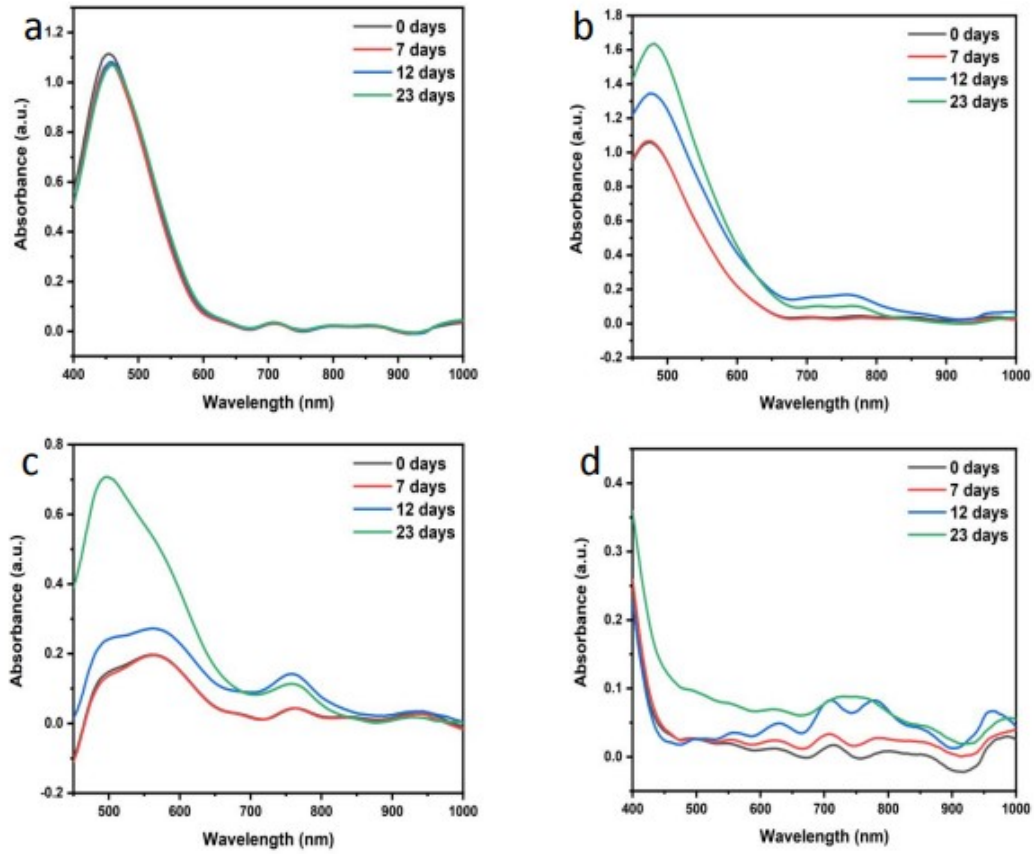

Figure S9. (a) UV-Vis spectra of LEG4|TiO_2, measured at various number of days after fabrication. The spectrum for mesoporous TiO_2 film was subtracted. (b) TiO_2|LEG4|TPABT on mesoporous TiO_2, measured at various number of days after fabrication. The spectrum for mesoporous TiO_2 film was subtracted. (c) TiO_2|LEG4|TPABT measured at various number of days after fabrication. The spectrum for mesoporous TiO_2|LEG4 was subtracted. (d) TPABT|TiO_2 only, measured at various number of days after fabrication. The spectrum for the mesoporous TiO_2 film was subtracted. The TPABT formulation was 50 mg ml^{-1} TPABT, 75 mM LiTFSI and 76 mM tBP.

Photoinduced Absorption Spectroscopy

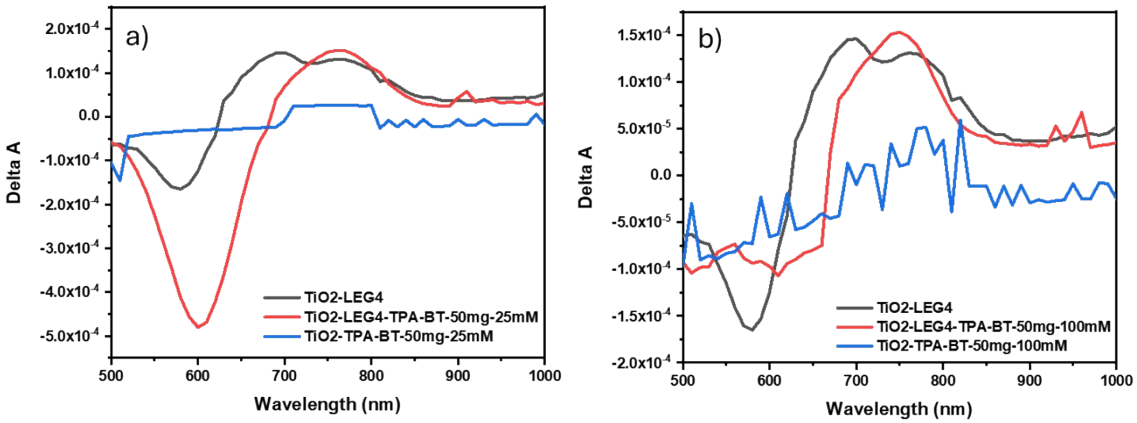

Figure S10. PIA spectra of LEG4|TiO_2, TPABT|TiO_2 and TPABT|LEG4|TiO_2 to show the difference between the spectrum for the photo-oxidised dye (LEG4|TiO_2) and the spectrum after regeneration of the dye by the HTM (Spiro-OMeTAD|LEG4|TiO_2). The TPABT concentration was 50 mg ml^{-1}. Left: LiTFSI concentration of 25 mM, right: LiTFSI concentration of 100 mM.

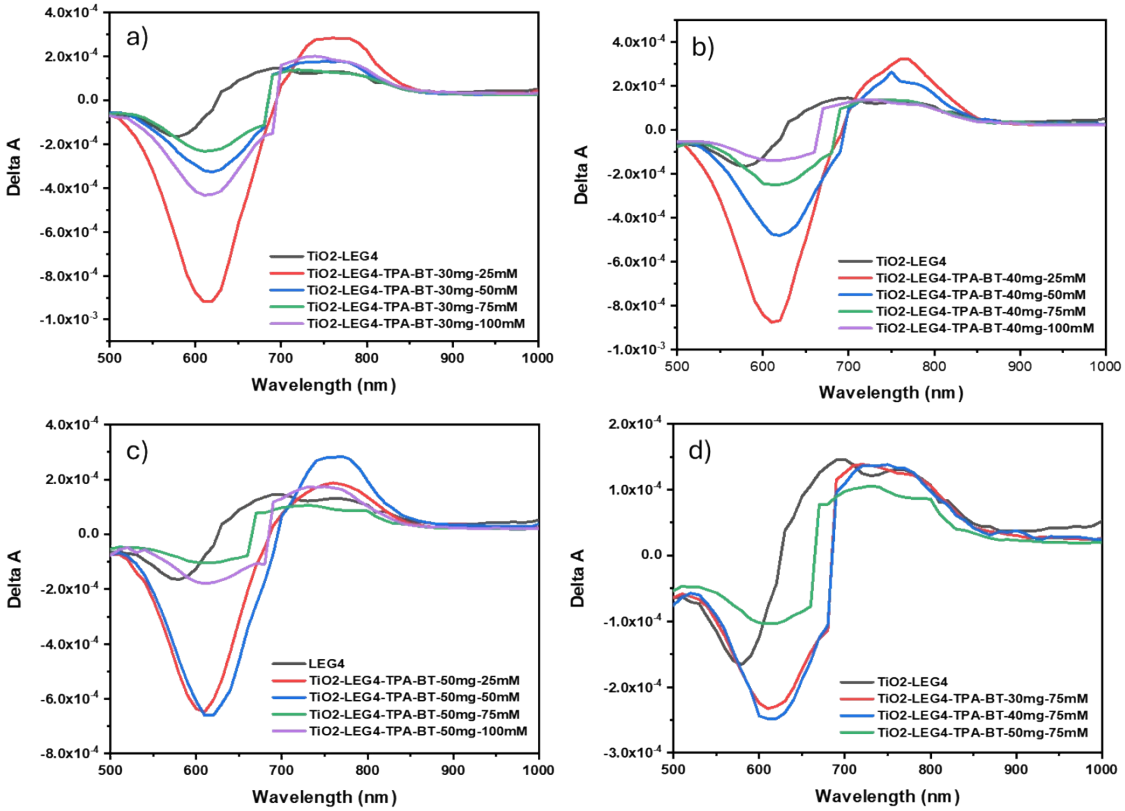

Figure S11. PIA spectra of fresh samples of LEG4|TiO_2, TPABT|TiO_2 to and TPABT|LEG4|TiO_2 on FTO glass with varying concentration of Li-TFSI added to TPABT and 76 mM tBP, for TPABT concentrations of a) 30 mg ml^{-1}, b) 40 mg ml^{-1} and c) 50 mg ml^{-1} and d) a comparison of varying concentration of TPABT at 75 mM LiTFSI.

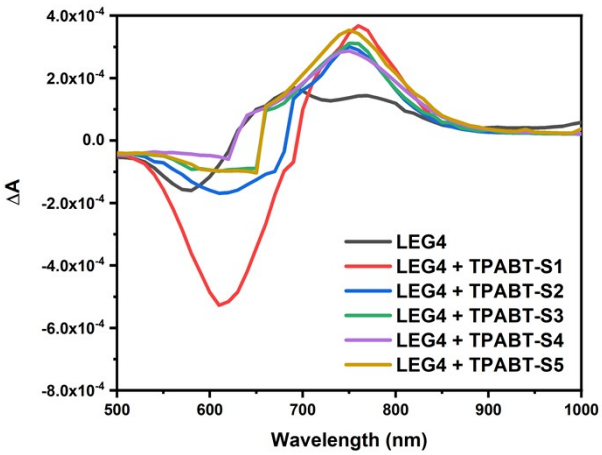

Figure S12. PIA spectra of two series of TPABT devices measured (a) 3 days after device fabrication. Sample series S (tBP:Li-TFSI = 1:0.33) contain increasing concentration of additives with increasing number in the series (See Table S1).

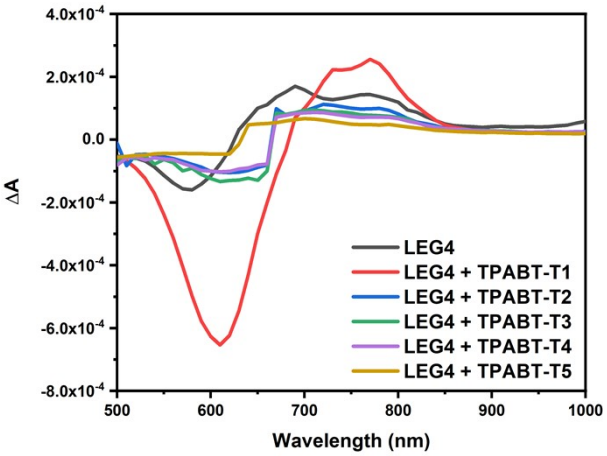

Figure S13. PIA spectra of two series of TPABT devices measured 23 days after device fabrication demonstrating how oxidation time affects dye regeneration. Sample series T (tBP:Li-TFSI = 1:0.22) contain increasing concentration of additives with increasing number in the series (see Table S1).

Transient Absorption Spectroscopy

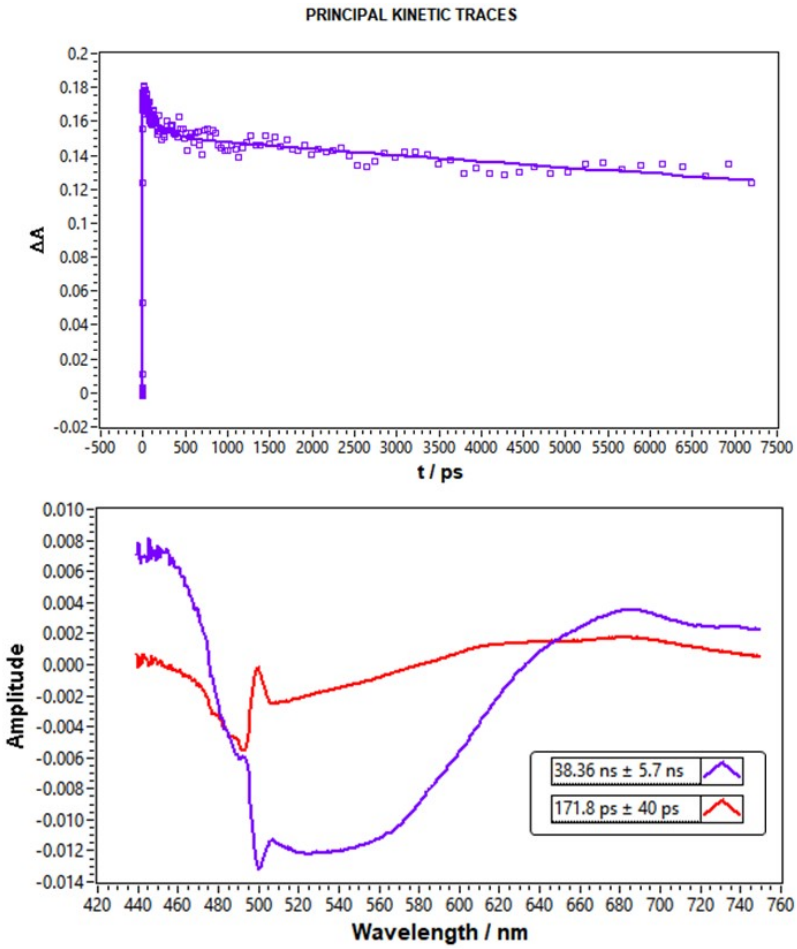

Figure S14. Global analysis Leg4|TiO_2 fs - ns.

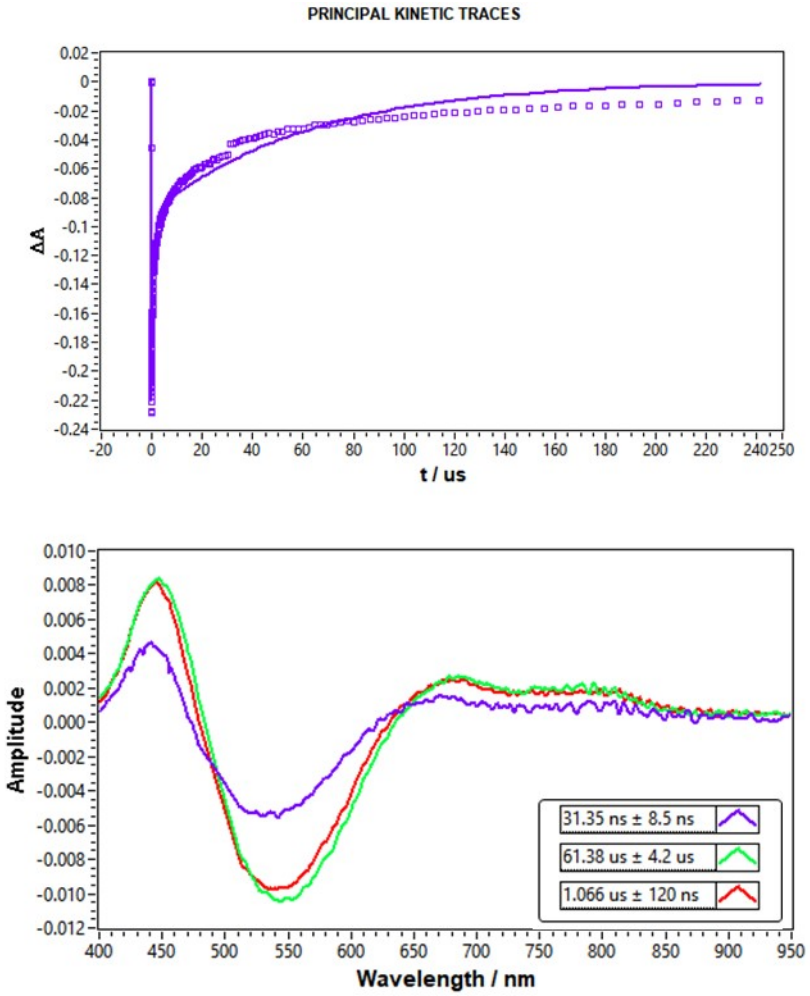

Figure S15. Global analysis Leg4|TiO_2 ns - µs.

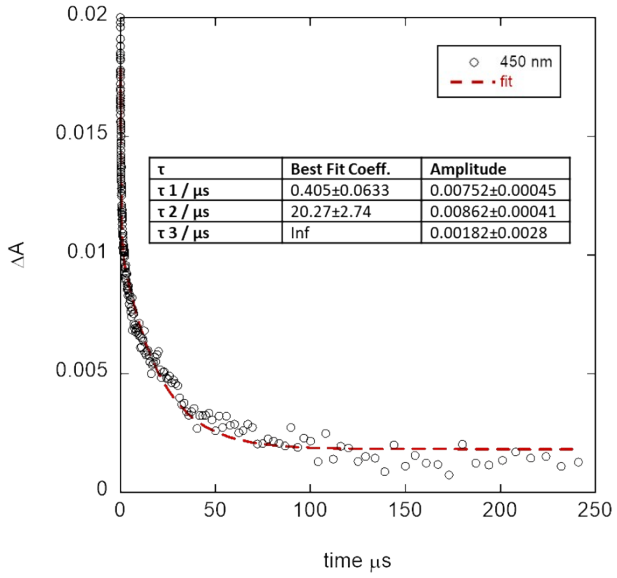

Figure S16. Linear fit of transient at 450 nm TiO_2| Leg4|Spiro-OMeTAD (25 mM LiTFSI, 76 mM tBP, 100 mg ml^{-1} Spiro-OMeTAD).

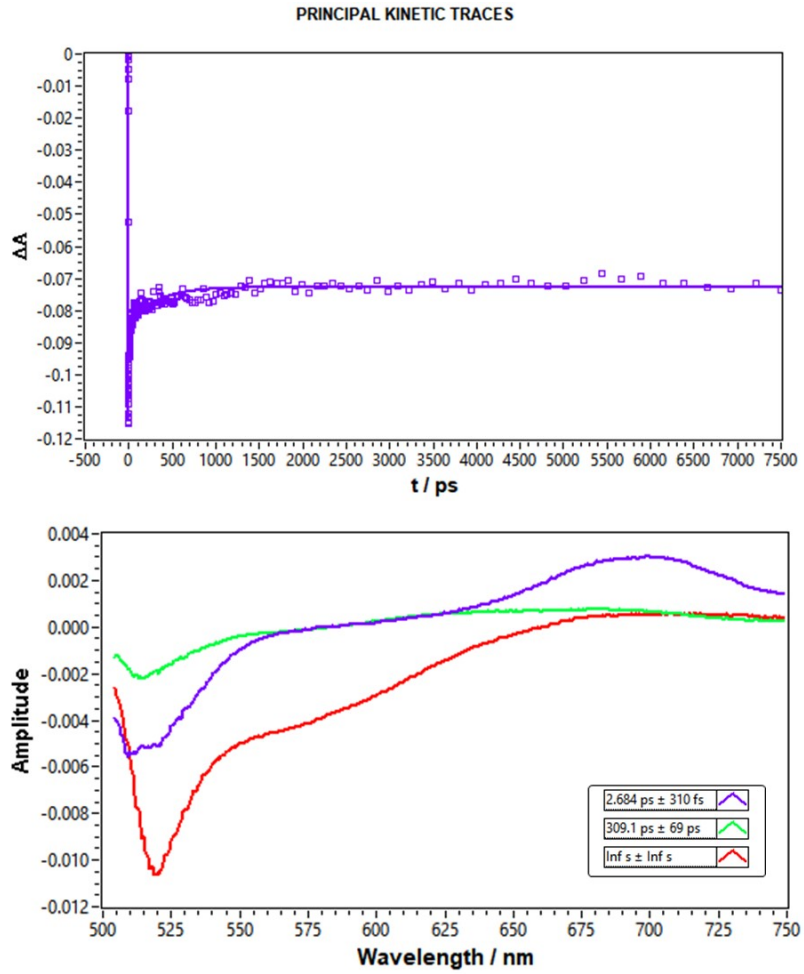

Figure S17. Global analysis TiO_2| Leg4|Spiro-OMeTAD (25 mM LiTFSI, 76 mM tBP, 100 mg ml^{-1} Spiro-OMeTAD).

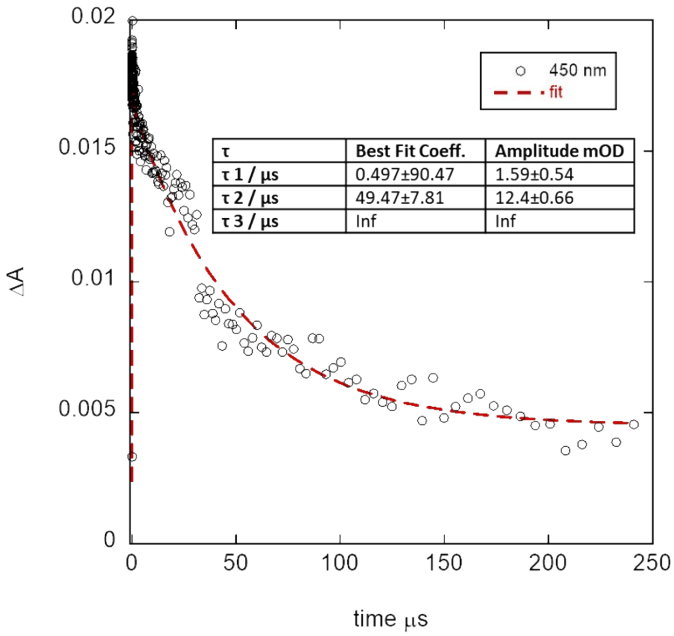

τ	Best Fit Coeff.	Amplitude mOD
τ 1 / μs	0.497±90.47	1.59±0.54
τ 2 / μs	49.47±7.81	12.4±0.66
τ 3 / μs	Inf	Inf

Figure S18. Linear fit of transient at 450 nm TiO_2| Leg4|Spiro-OMeTAD (25 mM LiTFSI, 76 mM tBP, 100 mg ml^{-1} Spiro-OMeTAD).

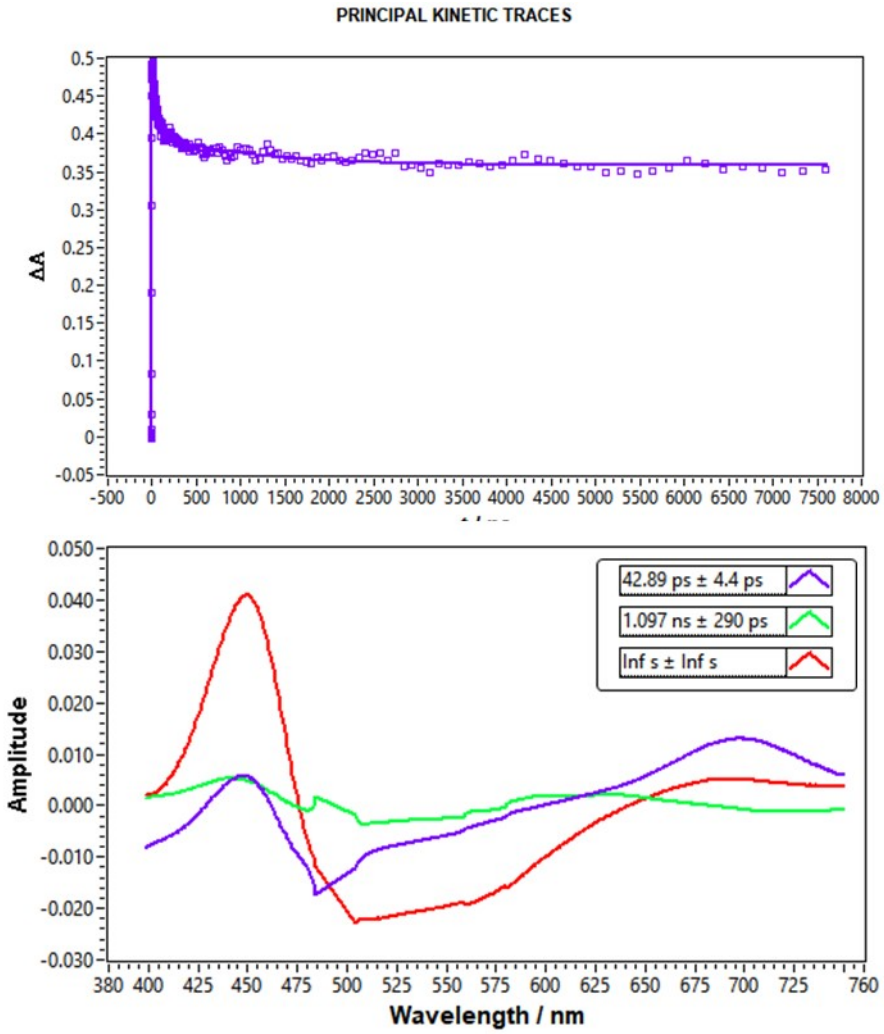

Figure S19. Global analysis TiO_2| Leg4|25 mM TPABT (25 mM LiTFSI, 76 mM tBP, 50 mg ml^{-1} TPABT) fs - ns

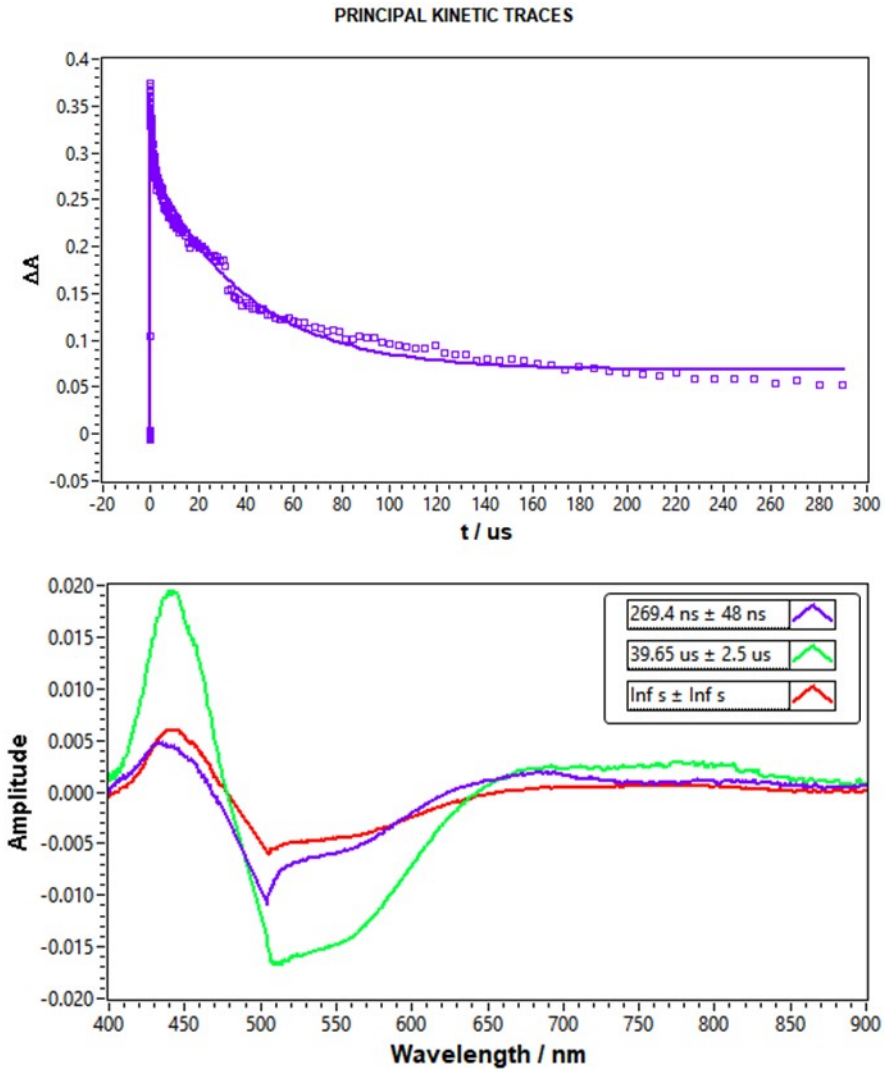

Figure S20. Global analysis TiO_2| Leg4|25 mM TPABT (25 mM LiTFSI, 76 mM tBP, 50 mg ml^{-1} TPABT) ns-µs.

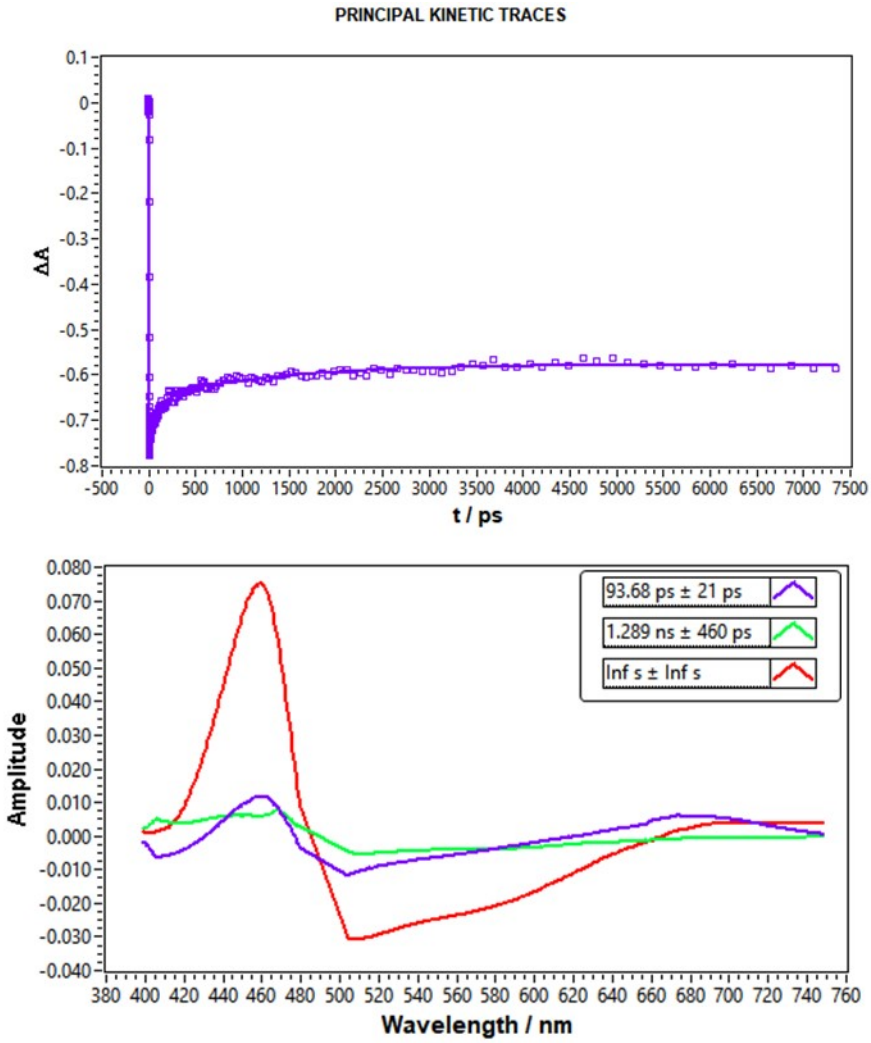

Figure S21. Global analysis TiO_2| Leg4|50 mM TPABT (50 mM LiTFSI, 76 mM tBP, 50 mg ml^{-1} TPABT) fs – ns.

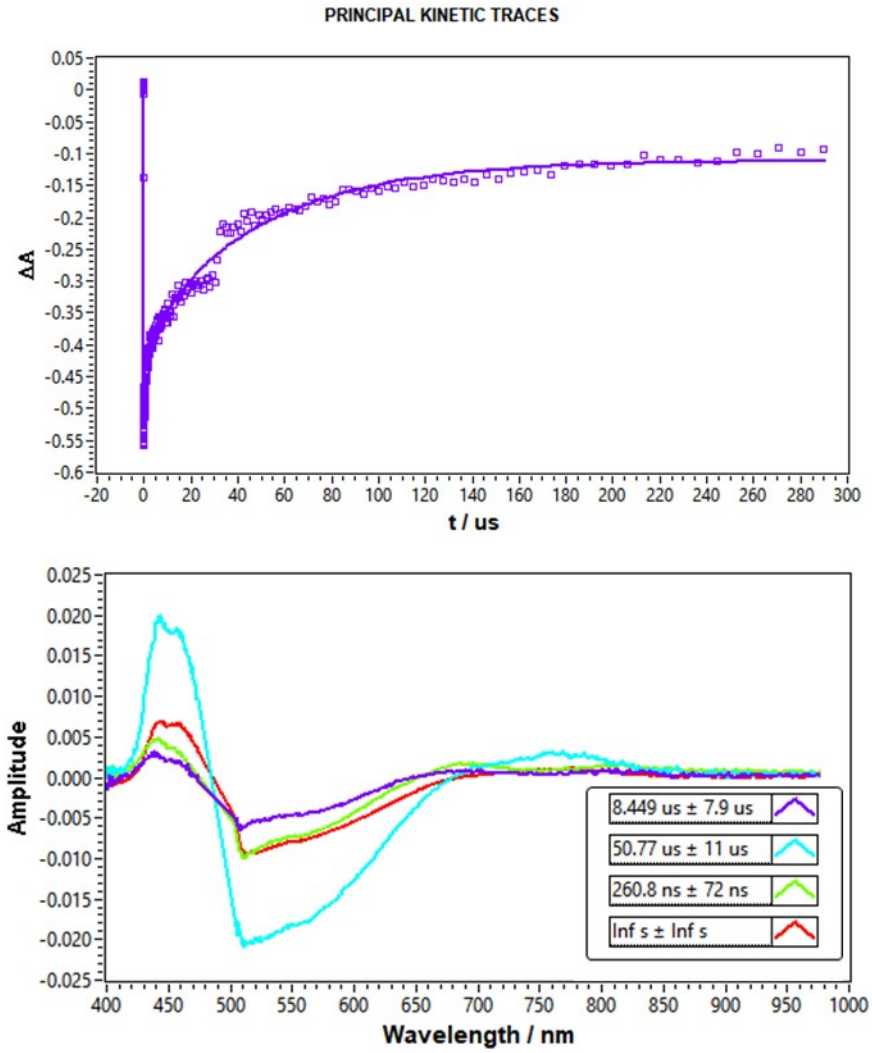

Figure S22. Global analysis TiO_2| Leg4|50 mM TPABT (50 mM LiTFSI, 76 mM tBP, 50 mg ml^{-1} TPABT) ns - µs.

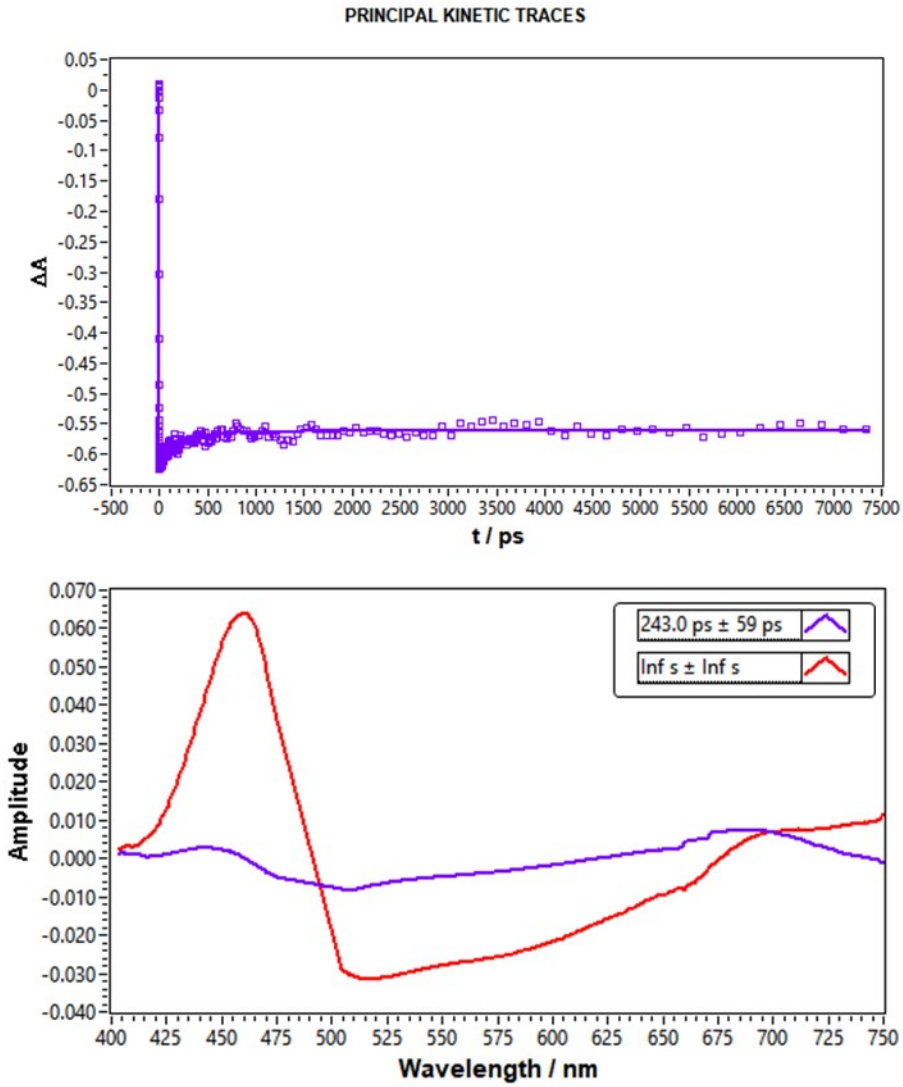

Figure S23. Global analysis TiO_2| Leg4|75 mM TPABT (7mM LiTFSI, 76 mM tBP, 50 mg ml^{-1} TPABT) fs – ns.

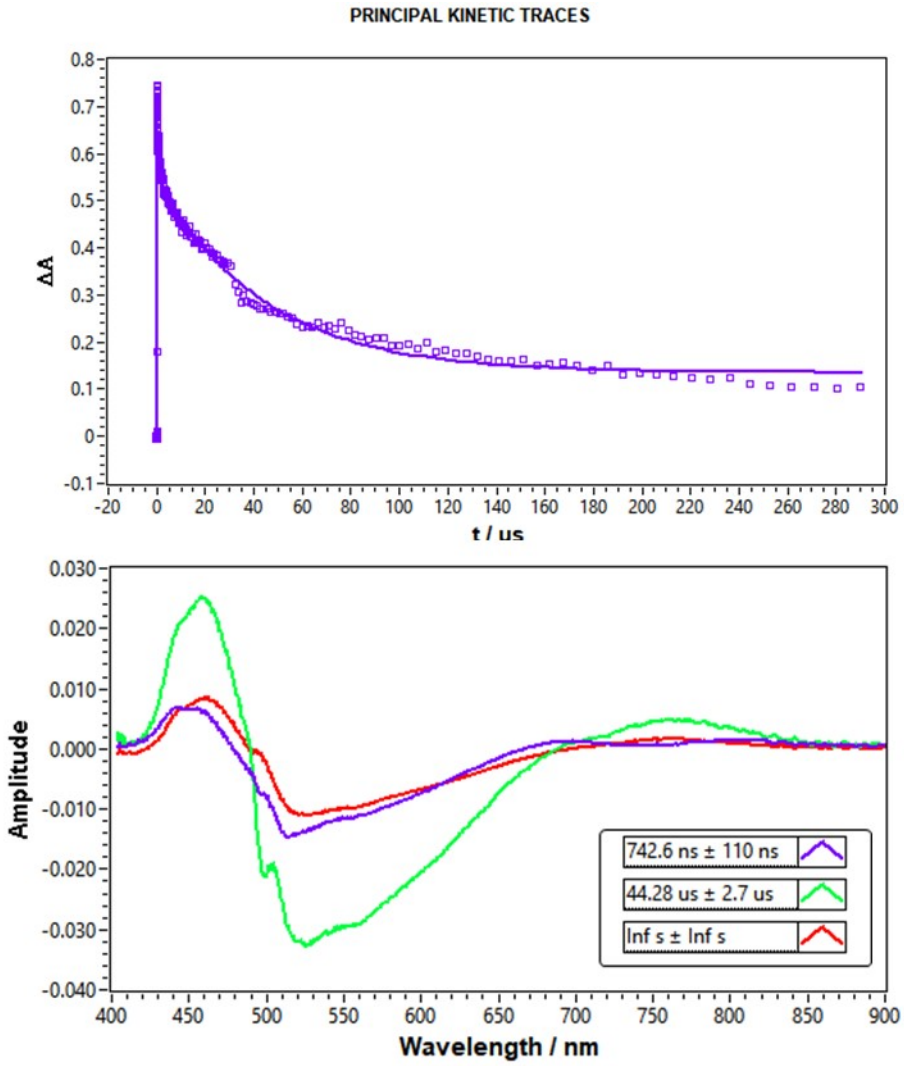

Figure S24. Global analysis TiO_2| Leg4|75 mM TPABT (75 mM LiTFSI, 76 mM tBP, 50 mg ml^{-1} TPABT) ns - µs.

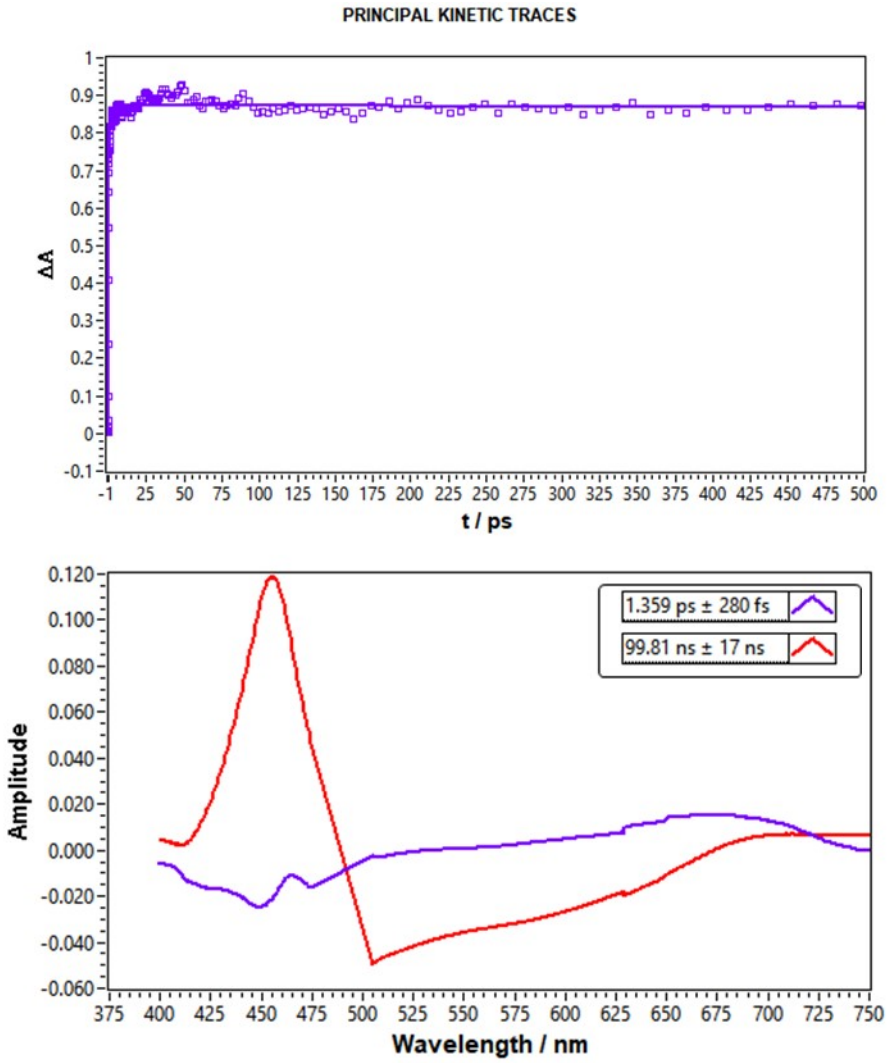

Figure S25. Global analysis TiO_2| Leg4|100 mM TPABT (100 mM LiTFSI, 76 mM tBP, 50 mg ml^{-1} TPABT) fs – ns.

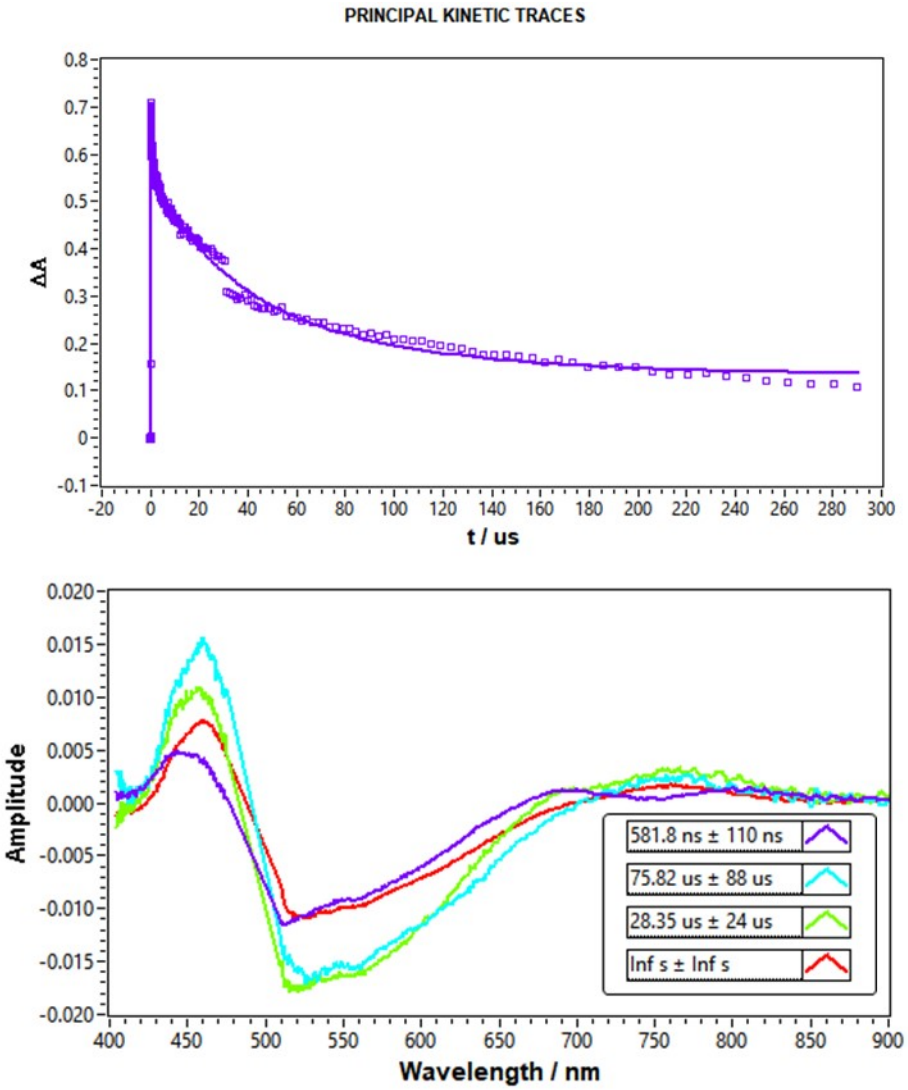

Figure S26. Global analysis TiO_2| Leg4|100 mM TPABT (100 mM LiTFSI, 76 mM tBP, 50 mg ml^{-1} TPABT) ns - µs.

Table S5. Summary of the lifetimes extracted from global analysis of the dye-sensitised films, after aging for 23 days, where 25-100 mM represents the concentration of LiTFSI added to TPABT (50 mg ml^{-1}) and tBP (76 mM).

Helios (< ns)					**Eos (> ns)**					
Sample	**[LiTFSI] / mM**	**t1 / ps**	**t2 / ns**	**t3**	**Sample**	**[LiTFSI] / mM**	**t1 / ns**	**t2 / µs**	**t3 / µs**	**t4**
Leg4|TiO_2	0	172 ± 40	38 ± 6		Leg4|TiO_2	0	31.3 ± 8.5	1.07 ± 0.12	61.4 ± 4.24	
TiO_2|Leg4|TPABT	25	42.9 ± 4.4	1.10 ± 0.29	Inf.	TiO_2|Leg4|TPABT	25	269 ± 48	39.7 ± 2.4	inf.	
TiO_2|Leg4|TPABT	50	93.7 ± 21.0	1.29 ± 0.46	Inf.	TiO_2|Leg4|TPABT	50	261 ± 72	8.45 ± 7.91	50.8 ± 11.2	inf
TiO_2|Leg4|TPABT	75	243 ± 59	inf		TiO_2|Leg4|TPABT	75	743 ± 106	44.3 ± 2.69	inf.	
TiO_2|Leg4|TPABT	100	1.36 ± 0.28	99.8 ± 17		TiO_2|Leg4|TPABT	100	582 ± 105	28.4 ± 24.3	75.8 ± 88.0	inf

Summary of ssDSSCs utilising dopant incorporated HTMs

Table S6. Photovoltaic parameters of ssDSSCs incorporating doped hole transporting materials.

Device architecture	**HTM**	**V_{OC} (V)**	**J_{SC} (mA cm^{-2})**	**FF**	**PCE (%)**	**Ref**
FTO/TiO_2/LEG4/TPABT/Ag	TPABT + tBP+ LiTFSI	0.71	4.9	0.65	2.3	This work
FTO/TiO_2/LEG4/Spiro-OMeTAD/Ag	Spiro-OMeTAD + tBP+ LiTFSI	0.86	8.9	0.62	4.7	[2]
FTO/TiO_2/LEG4/MeO-TPD/Ag	MeO-TPD + tBP + LiTFSI	0.80	9.5	0.65	4.9	[2]
FTO/TiO_2/LEG4/Spiro-OMeTAD/Ag	Spiro-OMeTAD + tBP+ LiTFSI + TeCA	0.90	11.7	0.73	7.7	[3]
FTO/TiO_2/LEG4/Spiro-OMeTAD/Ag	Spiro-OMeTAD + tBP + LiTFSI + FK209	0.97	9.8	0.71	6.8	[3]
FTO/TiO_2/Y123/Spiro-OMeTAD/Ag	Spiro-OMeTAD + tBP + LiTFSI + FK102	0.99	9.5	0.76	7.2	[4]
FTO/TiO_2/Y123/Spiro-OMeTAD/Ag	Spiro-OMeTAD + tBP + LiTFSI + TEMPO-Br	0.92	11.6	0.64	6.8	[5]
FTO/TiO_2/Y123/Spiro-OMeTAD/Ag	Spiro-OMeTAD + tBP + LiTFSI + DDQ	0.92	11.1	0.62	6.4	[6]
FTO/TiO_2/A2-F/Spiro-OMeTAD/Ag	Spiro-OMeTAD + LiTFSI + F4TCNQ	0.89	11.0	0.55	5.4	[7]
FTO/TiO_2/LEG4/X50/Ag	X50 + tBP + LiTFSI	0.88	10.3	0.75	6.8	[8]
FTO/TiO_2/LEG4/X60/Ag	X60 + tBP + LiTFSI	0.89	11.4	0.72	7.3	[9]

References

1 E. A. A. Alkhudhayr, D. Sirbu, M. Fsadni, B. Vella, B. T. Muhammad, P. G. Waddell, M. R. Probert, T. J. Penfold, T. Hallam, E. A. Gibson and P. Docampo, *ACS Appl Energy Mater*, 2023, **6**, 11573–11582.

2 L. Yang, B. Xu, D. Bi, H. Tian, G. Boschloo, L. Sun, A. Hagfeldt and E. M. J. Johansson, *J Am Chem Soc*, 2013, **135**, 7378–7385.

3 B. Xu, E. Gabrielsson, M. Safdari, M. Cheng, Y. Hua, H. Tian, J. M. Gardner, L. Kloo and L. Sun, *Adv Energy Mater*, 2015, **5**, 1402340.

4 J. Burschka, A. Dualeh, F. Kessler, E. Baranoff, N.-L. Cevey-Ha, C. Yi, M. K. Nazeeruddin and M. Grätzel, *J Am Chem Soc*, 2011, **133**, 18042–18045.

5 X. Yang, W. Wang, Y. Zhang and L. Sun, *Solar Energy*, 2018, **170**, 1001–1008.

6 W. Wang, X. Yang, J. Li, H. Wang, J. An, L. Zhang, X. Jiang, Z. Yu and L. Sun, *Energy Technology*, 2018, **6**, 752–758.

7 D.-Y. Chen, W.-H. Tseng, S.-P. Liang, C.-I. Wu, C.-W. Hsu, Y. Chi, W.-Y. Hung and P.-T. Chou, *Physical Chemistry Chemical Physics*, 2012, **14**, 11689.

8 L. Wang, E. Sheibani, Y. Guo, W. Zhang, Y. Li, P. Liu, B. Xu, L. Kloo and L. Sun, *Solar RRL*, 2019, **3**, 1900196.

9 B. Xu, D. Bi, Y. Hua, P. Liu, M. Cheng, M. Grätzel, L. Kloo, A. Hagfeldt and L. Sun, *Energy Environ Sci*, 2016, **9**, 873–877.